

Functionalization of Single-Walled Carbon Nanotubes with Polystyrene via Grafting to and Grafting from Methods

Shuhui Qin,[†] Dongqi Qin,[†] Warren T. Ford,^{*,†} Daniel E. Resasco,[‡] and Jose E. Herrera[‡]

Department of Chemistry, Oklahoma State University, Stillwater, Oklahoma 74078, and the School of Chemical Engineering and Materials Science, University of Oklahoma, Norman, Oklahoma 73019

Received August 15, 2003; Revised Manuscript Received November 20, 2003

ABSTRACT: Single-walled carbon nanotubes (SWNT) were functionalized with polystyrene (PSt) by grafting to and grafting from methods. PSt-N₃ with designed molecular weight and narrow molecular weight distribution was synthesized by atom transfer radical polymerization (ATRP) of styrene (St) followed by end group transformation and then added to SWNT. The grafting from functionalization was achieved by ATRP of St using 2-bromopropionate groups immobilized SWNT as initiator. Methyl 2-bromopropionate (MBP) was added as free initiator to control the chain propagation on SWNT during the polymerization. Raman and near-IR spectra show that PSt was covalently attached to the sidewalls of SWNT by the grafting to approach, and the degree of functionalization was about 1 in 48 SWNT carbon atoms as determined by thermogravimetric analyses (TGA). In the grafting from approach, size exclusion chromatography (SEC) results show that the molecular weight of free St increased linearly with St conversion, and the PSt cleaved from the SWNT after high conversion had the same molecular weight as the PSt produced in solution. TGA show that the amount of PSt grafted from the SWNT increased linearly with the molecular weight of the free PSt. By both methods, the final functionalized SWNT dissolved well in organic solvents, and the original SWNT bundles were broken into very small ropes or even individual tubes as revealed by AFM.

Introduction

Single-walled carbon nanotubes (SWNT) are one of the most striking recent discoveries in chemistry and materials science.¹ Their outstanding mechanical and electrical properties are leading to the development of new nanotechnologies.^{2–4} Functionalization of SWNT is important because the manipulation and processing of SWNT have been limited by insolubility in most common solvents.⁵ Both noncovalent and covalent modifications of the surface have been developed to improve solubility. Noncovalent chemistry includes surfactant modification,^{6–8} polymer wrapping,^{9–11} and polymer absorption^{12,13} in which the polymers were produced by an in situ ring-opening metathesis polymerization or emulsion polymerization. Covalent functionalization can be realized by either modification of carboxylic acid groups on the SWNT or direct addition of reagents to the sidewalls of SWNT. Carboxylic acid groups are introduced at the defect sites of SWNT by nitric acid oxidation, and long alkyl chains, polymers, and sugars have been attached by esterification and amidation reactions.^{14–18} Reagents added to the sidewalls include fluorine,¹⁹ aryl radicals,²⁰ aryl cations,²¹ hydrogen,²² nitrenes,²³ carbenes,^{23,24} radicals,^{4,25} and 1,3-dipoles.²⁶ These functionalizations improve the solubility and processability of SWNT but also alter the structure and electronic properties of SWNT.

Functionalization of SWNT with polymers is important because the long polymer chains will help the tubes dissolve in good solvents even with a low degree of functionalization. Furthermore, covalent attachment of polymers will help to disperse SWNT bundles. Dispersion of the SWNT into high aspect ratio small bundles

or individual tubes increases the tensile modulus and strength of SWNT–polymer composites. Recently, living anionic polymerization of St from SWNT was reported.²⁷ Here we report the functionalization of SWNT with PSt by the methods shown in Schemes 1 and 2. End group functionalized PSt (PSt-N₃) adds to SWNT via a cycloaddition reaction, and PSt grows from initiator functionalized SWNT by atom transfer radical polymerization (ATRP).

Experimental Section

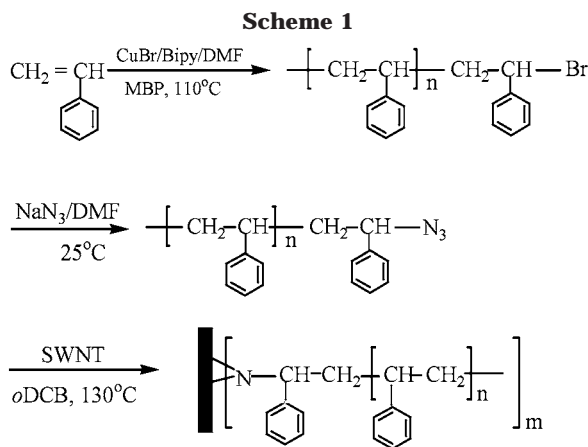
Materials. Styrene (Aldrich, 99%) was purified by passing through basic alumina and vacuum-distilled before use. Methyl 2-bromopropionate (MBP) (Aldrich, 98%), 2,2'-bipyridine (bipy) (Aldrich, 99+%), and sodium azide (Aldrich, 99%) were used as received. CuBr (Aldrich, 98%) was purified by stirring over glacial acetic acid (Fisher Scientific), followed by filtration and washing of the solid three times with ethanol and twice with diethyl ether, and vacuum-dried overnight. *N,N*-Dimethylformamide (DMF), 1,2-dichlorobenzene (DCB), and other solvents were used as received from Aldrich or Acros Chemicals. Single-walled carbon nanotubes were purchased from Carbon Nanotechnologies Inc., Houston, TX (HiPco, batch CM260015-6), and purified by oxidation with 2.6 M nitric acid.²⁸ All functionalization reactions employed the nitric acid-treated SWNT. Initiator immobilized SWNT (SWNT-initiator) with 4.1 initiator groups per 1000 carbons was synthesized as before.²⁹

Instruments and Measurements. Molecular weights were measured by SEC on an Agilent series 1100 chromatograph using THF as eluent (1 mL/min) at 40 °C with differential refractive index detection and two Polymer Laboratories columns (PL gel 10 μm mixed B, 7.5 mm i.d., linear range 10 000 000–500). Polystyrene standards in the range 1800 000–500 g/mol were used for calibration. TGA data were obtained in a nitrogen atmosphere with a Shimadzu TGA50/50H thermogravimetric analyzer. NMR spectra were recorded from CDCl₃ solutions on a 300 MHz Varian Gemini spectrometer. Raman spectra were recorded on thin films evaporated from DCB solutions onto glass using a Jovin Yvon-Horiba Lab Raman spectrometer equipped with a CCD detector and 633

* Corresponding author: e-mail wtford@okstate.edu.

[†] Oklahoma State University.

[‡] University of Oklahoma.



nm excitation.³⁰ Near-IR spectra were recorded on the same samples as the Raman spectra using a Bruker Equinox 55 FTIR/FTNIR instrument. Atomic force micrographs were obtained using a Multimode Nanoscope IIIa SPM (Digital Instruments, St. Barbara, CA) operating in the tapping mode. The samples for AFM measurements were prepared by spin-casting of a dilute solution of functionalized SWNT in DCB on a rotating mica surface at 2000 rpm.

Synthesis of PS-Br. A 25 mL dried Schlenk flask containing bipy (0.625 g, 4.00 mmol) was evacuated and refilled with nitrogen three times. Deoxygenated St (10.4 g, 0.100 mol) and 2 mL of DMF were added via syringe, and the reaction mixture was degassed by three freeze-pump-thaw cycles. After stirring for 1 h at room temperature CuBr (287 mg, 2.00 mmol) was added, and the flask was placed in a thermostated oil bath at 110 °C. After 3 min MBP (0.334 g, 2.00 mmol) was injected. After 4 h the polymerization was stopped at 62% conversion by cooling to room temperature and opening the flask to air. The mixture was dissolved into 120 mL of THF, passed through a column of neutral alumina, and precipitated into 900 mL of methanol. After filtration and vacuum-drying 5.8 g of white powder was collected. The ¹H NMR spectrum showed a peak at 4.4 ppm, assigned to the -CH(Ph)-Br end group. The molecular weight was calculated from the ¹H NMR spectrum ($M_n = 3350$) and was measured by SEC ($M_n = 3270$ and $M_w/M_n = 1.10$).

Transformation of PS-Br to PS-N₃.³¹ In a 50 mL round-bottomed flask PS-Br (4.19 g, 1.3 mmol), NaN₃ (0.088 g, 2.0 mmol), and 30 mL of DMF were stirred at 25 °C for 12 h. The reaction mixture was precipitated into 200 mL of methanol, and the white precipitate was collected by filtration. The solid was washed with deionized water three times to remove NaBr and unreacted NaN₃. The white powder was dried in a vacuum and stored at -5 °C. The complete substitution of the Br end group by the N₃ group was proved by the ¹H NMR spectrum in which the signal assigned to the -CH(Ph)-Br end group

at 4.4 ppm disappeared completely, and a new peak due to the -CH(Ph)-N₃ end group appeared at 4.0 ppm. The molecular weight was calculated to be 3370 from the ¹H NMR spectrum.

Addition of PS-N₃ to SWNT. A 50 mL round-bottomed flask was charged with SWNT (15 mg), PS-N₃ (1.0 g), and DCB (25 mL). After stirring 10 h at room temperature to form a black suspension, the flask was fitted with a condenser and the mixture was stirred at 130 °C under nitrogen for 60 h. After cooling to room temperature, the mixture was diluted with 150 mL of DCB, bath sonicated for 1 h, and filtered through a 0.2 μm PTFE membrane. The solid was washed with DCB to remove soluble PS. After 10 washings there was no cloudiness when 5 drops of colorless filtrate was added to 10 mL of methanol, indicating that little or no soluble PS remained. A pale gray solid was obtained after vacuum-drying at 100 °C for 30 h.

Grafting PS from SWNT. A 50 mL dried Schlenk flask containing SWNT-initiator (15 mg, 0.0050 mmol of initiator groups) and bipy (32.8 mg, 0.210 mmol) was degassed and refilled with nitrogen three times. Deoxygenated St (5.46 g, 52.5 mmol) and 4 mL of DCB were added, and the reaction mixture was degassed by four freeze-pump-thaw cycles. After stirring for 1 h at room temperature, CuBr (15.1 mg, 0.105 mmol) was added, and the flask was placed in a thermostated oil bath at 110 °C. After 3 min, MBP (16.7 mg, 0.1 mmol) was injected, and an initial kinetic sample was taken. During the polymerization samples were removed to analyze conversion by peak areas of monomer and polymer in ¹H NMR spectra and to analyze molecular weight by SEC. After 14 h the polymerization was stopped at 76% conversion, and the PS-SWNT was isolated by the method of the preceding paragraph.

Cleavage of PS from SWNT. A 50 mL round-bottomed flask was charged with 15 mg of SWNT-*g*-PS, 10 mL of DCB, 4.5 mL of 1-butanol, and 0.5 mL of concentrated sulfuric acid. The flask was fitted with a water condenser, and the mixture was stirred at 95–100 °C for 7 days. The solvent was removed under vacuum, and the residue was dispersed in 10 mL of chloroform. After an extraction with 3 mL of water, the organic phase was isolated, and the solvent was distilled off. The remaining solid was dispersed in anhydrous THF, SWNT were removed by filtration through a 0.2 μm PTFE membrane, and the molecular weight of PS in the filtrate was analyzed by SEC.

Results and Discussion

Grafting Polystyrene to SWNT. Addition of a nitrene, which is formed by thermolysis of an azide group, to the strained double bonds of [60]fullerene (C₆₀) is an excellent method for preparation of C₆₀ derivatives.^{32,33} This cycloaddition reaction was applied to synthesize on-chain polymeric C₆₀ and C₆₀ end-capped polymer.^{34,35} Since SWNT also have strained double bonds (but less strained than those of C₆₀), addition of PS with an azido end group should be a method for SWNT functionalization.

Well-defined PS-N₃ was prepared by ATRP of St followed by end group transformation as shown in Scheme 1. The ATRP of St at 110 °C, using MBP as an initiator and CuBr/bipy complex as a catalyst, was stopped at 62% conversion after 4 h. The PS-Br was converted to PS-N₃ with sodium azide in DMF. The ¹H NMR spectrum showed complete conversion of PS-Br to PS-N₃. Almost the same value of $M_n = 3300$ was determined by both ¹H NMR and SEC analysis, which indicates that the end group functionality of both PS-Br and PS-N₃ was about one reactive end group per polymer chain.

The cycloaddition reaction was carried out by stirring a mixture of PS-N₃ and SWNT in DCB at 130 °C in a nitrogen atmosphere for 60 h. The purified product was

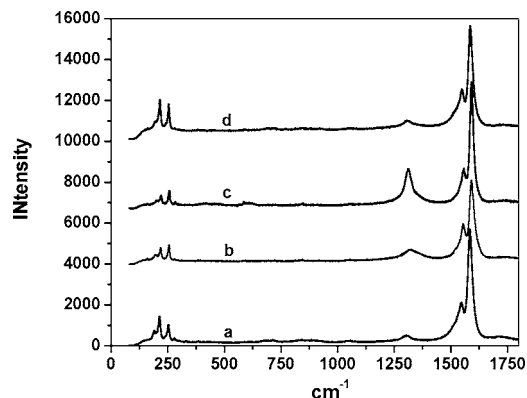


Figure 1. Raman spectra of pristine HiPco SWNT (a), nitric acid-treated SWNT (b), SWNT-*g*-PSt (c), and SWNT after TGA of SWNT-*g*-PSt (d).

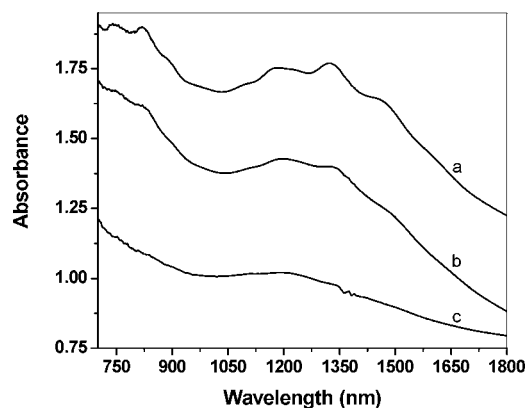


Figure 2. NIR spectra of pristine HiPco SWNT (a), nitric acid-treated SWNT (b), and SWNT-*g*-PSt (c).

a pale gray solid that dissolves in organic solvents such as DCB, DMF, and CHCl_3 . TGA gave 85% weight loss in a nitrogen atmosphere at 800 °C, indicating that the composite contained 85% PSt and 15% SWNT. The degree of functionalization was 1 PSt chain per 48 SWNT carbons calculated from the PSt molecular weight and the TGA result.

Raman spectroscopy gives direct evidence for covalent sidewall functionalization as shown in Figure 1. Pristine and nitric acid-treated HiPco SWNT exhibit weak diameter-dependent radial breathing (ω_r) mode bands at 180–260 cm^{-1} and a strong tangential (ω_t) mode band at 1590 cm^{-1} . The disorder mode band around 1295 cm^{-1} attributed to sp^3 -hybridized carbon in the hexagonal framework of the nanotube walls is very weak (Figure 1a,b). The disorder mode band is enhanced significantly after reaction with PSt- N_3 (Figure 1c), indicating that more sp^3 -hybridized carbons were produced by functionalization; however, the bands corresponding to the radial breathing mode are still present, indicating that the structure of the SWNT remains basically intact. After TGA of this PSt functionalized SWNT, the Raman spectrum was about the same as that of pristine SWNT, as seen in Figure 1a,d. Thus, the Raman results show that PSt was covalently attached to the sidewalls of SWNT and then detached by heating to 800 °C.

Near-IR spectroscopy demonstrates the covalent sidewall functionalization, too. The spectrum of the pristine HiPco SWNT (Figure 2a) contains a good deal of structure from the van Hove transitions at 1400 nm to 800 nm, which are attributed to first and second band

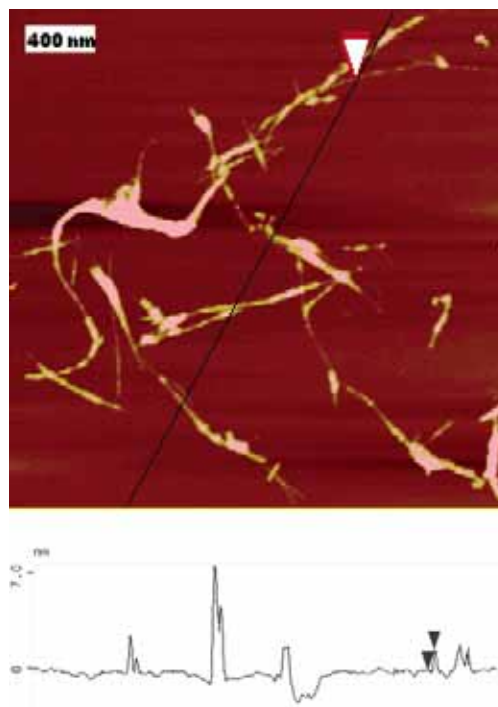


Figure 3. AFM height image of SWNT-*g*-PSt prepared by the grafting to method. The height shown by the arrows is 1.6 nm.

gap transitions in semiconducting nanotubes. The band frequencies depend on the tube diameter and chirality, and each band might represent a set of nanotubes with similar diameters.³⁶ The intensity of these bands is weaker but still present in nitric acid-treated SWNT (Figure 2b). These bands are lost completely, and a smooth curve appears in the near-IR spectrum of the functionalized SWNT as shown in Figure 2c. The result supports covalent attachment of PSt which greatly modifies the electronic structure of SWNT.

The tapping mode AFM height image in Figure 3 shows that the functionalized tubes are individual SWNT and very small bundles. The heights of tubes range from 0.8 to 6.2 nm with an average of 2.5 nm from 40 measurements. The tubes and tube bundles are 500–2500 nm in length. The contours of functionalized SWNT are of different diameter even in one bundle, indicating that bundles contain tubes of different lengths or that the PSt clumps on the surface of the SWNT as the DCB evaporates. In related work on poly(*n*-butyl methacrylate) (PnBMA) brushes having SWNT backbones,²⁹ the PnBMA, having a low T_g , spread on a mica surface. In contrast, the PSt, having a higher T_g , hardened on the sidewalls of SWNT due to stronger interaction between PSt and SWNT than between PSt and mica.

Grafting Polystyrene from SWNT. PSt grows from SWNT by ATRP initiated with bromopropionate groups immobilized on SWNT (SWNT-initiator) as shown in Scheme 2. The SWNT-initiator had one initiator group per 240 carbon atoms of SWNT. The advantage of this method is that the chain length of PSt can be controlled well by ATRP, and thus the solubility of functionalized SWNT can be controlled. The polymerization was carried out in DCB at 110 °C, and MBP was added as a free initiator to control the chain propagation from solid surface and to monitor the polymerization kinetics.

Figure 4 shows the kinetics of the polymerization and evolution of M_n and M_w/M_n of the free PSt produced in

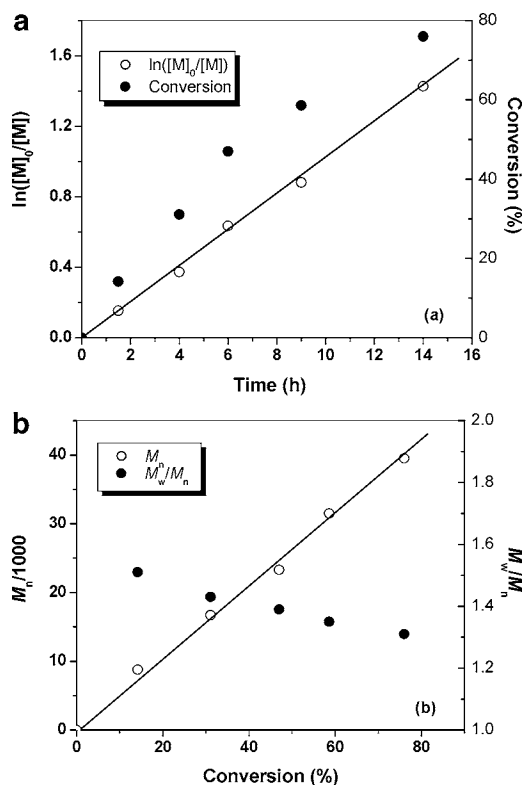


Figure 4. Dependences of $\ln([M]_0/[M])$ and conversion on time (a) and M_n and M_w/M_n on conversion (b) during the SWNT-*g*-PSt synthesis. Conditions: [St]:[initiator]:[CuBr]:[Bipy] = 500:1:1:2 in dichlorobenzene at 110 °C; initiator = SWNT-initiator + MBP with [SWNT-initiator]/[MBP] = 1/20.

the solution. The semilogarithmic kinetic plot is linear and passes through the origin, demonstrating that the number of active propagating species is constant throughout the polymerization and that the kinetics are first order in monomer concentration. The molecular weights measured by SEC increase linearly with monomer conversion, and the polydispersity of the free polymer is rather low in all cases ($M_w/M_n = 1.31$ at 76% conversion). Therefore, the ATRP of St initiated by free initiator, MBP, is a controlled/living process.

The solubility of the SWNT-*g*-PSt taken out during the polymerization depends on the chain length of the polymer. For example, the sample taken out after 14.2% monomer conversion disperses well in DCB as a stable black suspension but precipitates in THF. The sample after 47% monomer conversion dissolves in DCB and suspends in THF. The final product (76% conversion) forms black solutions in DCB and THF. The solution of SWNT-*g*-PSt in DCB is stable for at least 5 months, while without attached polymer the SWNT precipitates in 10 min.

The relative amounts of grafted polymer and SWNT were determined by TGA. Figure 5 shows the thermograms of SWNT-initiator, SWNT-*g*-PSt, and PSt under nitrogen. All of the initiator moieties (Figure 5a) and bulk PSt (Figure 5f) are assumed to be lost at 800 °C, leaving residual SWNT. Figure 6 shows that the weight of grafted polymer increases linearly with M_n of the free polymer. Therefore, the number of graft sites on SWNT is almost constant during the course of polymerization; i.e., the growth of PSt from SWNT is controlled.

Free PSt was removed from the SWNT-*g*-PSt by extensive washing with DCB. The grafted PSt was cleaved from SWNT using acid-catalyzed transesterifi-

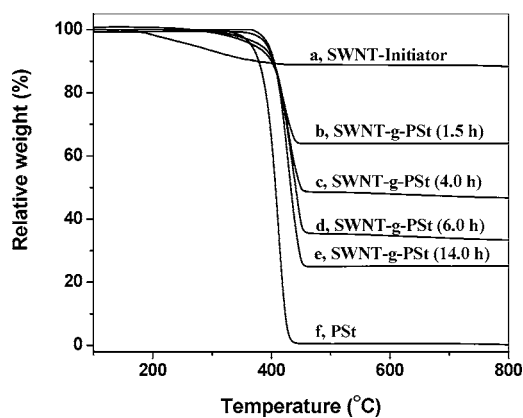


Figure 5. TGA thermograms of SWNT-initiator (a), SWNT-*g*-PSt taken at different time intervals (b, c, d, e), and PSt (f) under nitrogen. The weight percent left at 500 °C is (a) 88.8%, (b) 63.9%, (c) 48.5%, (d) 35.9%, (e) 24.8%, and (f) <0.8%.

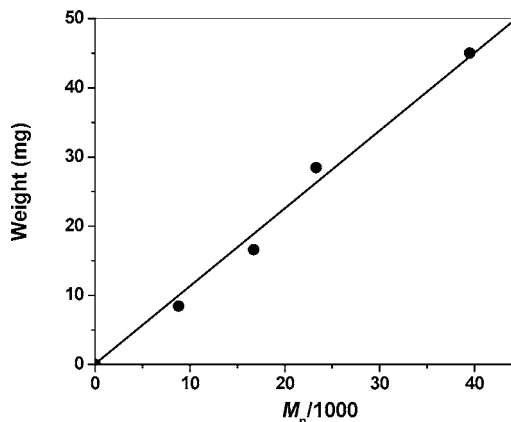


Figure 6. Relationship of amount of polymer grafted to SWNT and M_n of the free polymer produced in solution.

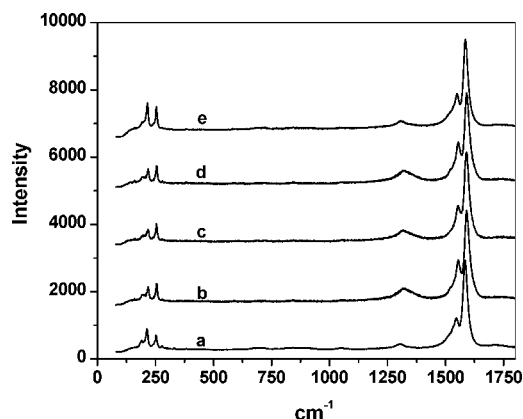


Figure 7. Raman spectra of pristine SWNT (a), nitric acid-treated SWNT (b), SWNT-initiator (c), SWNT-*g*-PSt (d), and SWNT-*g*-PSt after TGA (e).

cation in 1-butanol. The molecular weight of the cleaved PSt ($M_n = 3.41 \times 10^4$, $M_w/M_n = 1.38$) was close to that of the free PSt produced at the same time ($M_n = 3.75 \times 10^4$, $M_w/M_n = 1.31$), indicating that the growth of PSt from SWNT was the same as the PSt initiated with free MBP via ATRP.

Figure 7 shows the Raman spectra of pristine HiPco SWNT, nitric acid-treated SWNT, SWNT-initiator, SWNT-*g*-PSt, and the sample remaining after TGA of SWNT-*g*-PSt. The weak diameter-dependent radial breathing (ω_r) mode at 180–260 cm^{-1} and the strong tangential (ω_t) mode band at 1590 cm^{-1} are present in

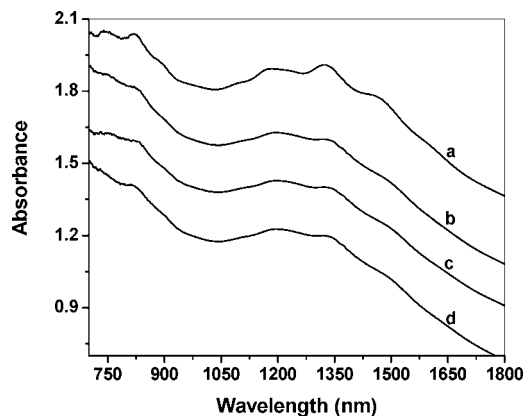


Figure 8. NIR spectra of pristine SWNT (a), nitric acid-treated SWNT (b), SWNT-initiator (c), and SWNT-*g*-PSt (d).

all cases. Compared with the very weak disorder mode around 1295 cm^{-1} in pristine SWNT (Figure 7a), this sp^3 mode increased a little in intensity (but was still weak) in the nitric acid-treated SWNT (Figure 7b). No further change of the Raman spectrum (Figure 7c,d) was found by initiator functionalization and growth of polymer from the SWNT-initiator. Furthermore, the intensity of the disorder mode band in Figure 7e decreased compared with that of SWNT-*g*-PSt, revealing that the sidewall structure of SWNT was recovered by removal of functionality by heating to $800\text{ }^\circ\text{C}$ under a nitrogen atmosphere in the TGA.

Near-IR spectra of pristine HiPco SWNT, nitric acid-treated SWNT, SWNT-initiator, and SWNT-*g*-PSt are shown in Figure 8. Compared with the spectrum of pristine SWNT (Figure 8a), which contains a good deal of structure, the intensity of the peaks in the spectrum of the nitric acid-treated SWNT (Figure 8b) is weaker. Furthermore, there is no significant change in peak intensity after functionalization with initiator and growth of PSt as shown in Figure 8c,d. The results indicate that the nitric acid oxidation produced some defects on the sidewalls of the SWNT, while conversion to ATRP initiator and grafting of PSt did not alter the structure of SWNT further.

A thin film of the SWNT-*g*-PSt sample on a mica surface was prepared by spin-coating, and its microstructure was analyzed by tapping mode AFM. The image in Figure 9 shows heights from 0.7 to 4.8 nm with an average height of 1.8 nm from 40 measurements. Thus, almost all of the tubes are individual or very small bundles. No big bundles were found. The final functionalized tubes dissolve well in common organic solvents such as DCB, DMF, and chloroform. Generally, samples of same PSt content prepared by grafting from and grafting to methods have similar solubility.

Conclusions

Single-walled carbon nanotubes (SWNT) can be functionalized with PSt by both grafting to and grafting from methods. Grafting to functionalization was realized by cycloaddition of PSt- N_3 to the sidewalls of SWNT. Covalent attachment was proved by Raman and near-IR spectra. TGA and the molecular weight of the PSt- N_3 showed that the functionalization density was 1 polystyrene chain per 48 carbon atoms of SWNT. Grafting from was realized by ATRP of St monomer from SWNT that were functionalized with one ATRP initiator per 240 carbon atoms of SWNT. Initiator functionalization and polymerization did not change the

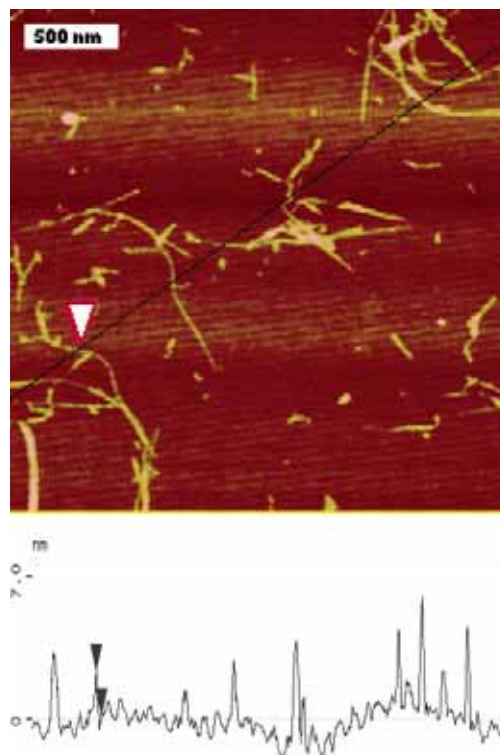


Figure 9. AFM height image of SWNT-*g*-PSt prepared by the grafting from method. The height shown by the arrows is 2.1 nm.

sidewall structures of the SWNT according to Raman and near-IR spectra. TGA showed that the amount of polymer grafted on SWNT increased with increasing reaction time and was proportional to the molecular weight of the free PSt obtained by initiation with free MBP at the same time. By both grafting methods, increasing the PSt content increased solubility in organic solvents, and the final functionalized tubes dissolved well. AFM showed that the original SWNT bundles were broken into very small ropes or even individual tubes by functionalization and polymerization.

Acknowledgment. Financial support from the National Science Foundation (EPS-0132543) is gratefully acknowledged. We thank LeGrande Slaughter for use of the TGA.

References and Notes

- (1) Dresselhaus, M. S.; Dresselhaus, G.; Avouris, P. *Carbon Nanotubes: synthesis, structure, properties and applications*; Springer-Verlag Press: Heidelberg, 2001.
- (2) Ajayan, P. M. *Chem. Rev.* **1999**, *99*, 1787–1799.
- (3) Dai, H. *Acc. Chem. Res.* **2002**, *35*, 1035–1044.
- (4) Hirsch, A. *Angew. Chem., Int. Ed.* **2002**, *41*, 1853–1859.
- (5) Baughman, R. H.; Zakhidov, A. A.; de Heer, W. A. *Science* **2002**, *297*, 787–792.
- (6) O'Connell, M. J.; Bachilo, S. M.; Huffman, C. B.; Moore, V. C.; Strano, M. S.; Haroz, E. H.; Rialon, K. L.; Boul, P. J.; Noon, W. H.; Kittrell, C.; Ma, J. P.; Hauge, R. H.; Weisman, R. B.; Smalley, R. E. *Science* **2002**, *297*, 593–596.
- (7) Islam, M. F.; Rojas, E.; Bergey, D. M.; Johnson, A. T.; Yodh, A. G. *Nano Lett.* **2003**, *3*, 269–273.
- (8) Kang, Y. J.; Taton, T. A. *J. Am. Chem. Soc.* **2003**, *125*, 5650–5651.
- (9) O'Connell, M. J.; Boul, P.; Ericson, L. M.; Huffman, C.; Wang, Y. H.; Haroz, E.; Kuper, C.; Tour, J.; Ausman, K. D.; Smalley, R. E. *Chem. Phys. Lett.* **2001**, *342*, 265–271.
- (10) Star, A.; Stoddart, J. F. *Macromolecules* **2002**, *35*, 7516–7520.

- (11) Star, A.; Stoddart, J. F.; Steuerman, D.; Diehl, M.; Boukai, A.; Wong, E. W.; Yang, X.; Chung, S. W.; Choi, H.; Heath, J. R. *Angew. Chem., Int. Ed.* **2001**, *40*, 1721–1725.
- (12) Gomez, F. J.; Chen, R. J.; Wang, D. W.; Waymouth, R. M.; Dai, H. *Chem. Commun.* **2003**, 190–191.
- (13) Barraza, H. J.; Pompeo, F.; O'Rear, E. A.; Resasco, D. E. *Nano Lett.* **2002**, *2*, 797–802.
- (14) Chen, J.; Hamon, M. A.; Hu, H.; Chen, Y. S.; Rao, A. M.; Eklund, P. C.; Haddon, R. C. *Science* **1998**, *282*, 95–98.
- (15) Sun, Y. P.; Fu, K. F.; Lin, Y.; Huang, W. J. *Acc. Chem. Res.* **2002**, *35*, 1096–1104.
- (16) Sano, M.; Kamino, A.; Okamura, J.; Shinkai, S. *Langmuir* **2001**, *17*, 5125–5128.
- (17) Niyogi, S.; Hamon, M. A.; Hu, H.; Zhao, B.; Bhowmik, P.; Sen, R.; Itkis, M. E.; Haddon, R. C. *Acc. Chem. Res.* **2002**, *35*, 1105–1113.
- (18) Pompeo, F.; Resasco, D. E. *Nano Lett.* **2002**, *2*, 369–373.
- (19) Mickelson, E. T.; Huffman, C. B.; Rinzler, A. G.; Smalley, R. E.; Hauge, R. H.; Margrave, J. L. *Chem. Phys. Lett.* **1998**, *296*, 188–194.
- (20) Bahr, J. L.; Yang, J. P.; Kosynkin, D. V.; Bronikowski, M. J.; Smalley, R. E.; Tour, J. M. *J. Am. Chem. Soc.* **2001**, *123*, 6536–6542.
- (21) Dyke, C. A.; Tour, J. M. *J. Am. Chem. Soc.* **2003**, *125*, 1156–1157.
- (22) Pekker, S.; Salvetat, J. P.; Jakab, E.; Bonard, J. M.; Forro, L. *J. Phys. Chem. B* **2001**, *105*, 7938–7943.
- (23) Holzinger, M.; Vostrowsky, O.; Hirsch, A.; Hennrich, F.; Kappes, M.; Weiss, R.; Jellen, F. *Angew. Chem., Int. Ed.* **2001**, *40*, 4002–4005.
- (24) Chen, Y.; Haddon, R. C.; Fang, S.; Rao, A. M.; Lee, W. H.; Dickey, E. C.; Grulke, E. A.; Pendergrass, J. C.; Chavan, A.; Haley, B. E.; Smalley, R. E. *J. Mater. Res.* **1998**, *13*, 2423–2431.
- (25) Ying, Y. M.; Saini, R. K.; Liang, F.; Sadana, A. K.; Billups, W. E. *Org. Lett.* **2003**, *5*, 1471–1473.
- (26) Georgakilas, V.; Kordatos, K.; Prato, M.; Guldi, D. M.; Holzinger, M.; Hirsch, A. *J. Am. Chem. Soc.* **2002**, *124*, 760–761.
- (27) Viswanathan, G.; Chakrapan, N.; Yang, H.; Wei, B.; Chung, H.; Cho, K.; Ryu, C. Y.; Ajayan, M. P. *J. Am. Chem. Soc.* **2003**, *125*, 9258–9259.
- (28) Liu, J.; Rinzler, A. G.; Dai, H. J.; Hafner, J. H.; Bradley, R. K.; Boul, P. J.; Lu, A.; Iverson, T.; Shelimov, K.; Huffman, C. B.; Rodriguez-Macias, F.; Shon, Y. S.; Lee, T. R.; Colbert, D. T.; Smalley, R. E. *Science* **1998**, *280*, 1253–1256.
- (29) Qin, S. H.; Qin, D. Q.; Ford, W. T.; Resasco, D. E.; Herrera, J. E. *J. Am. Chem. Soc.*, in press.
- (30) Herrera, J. E.; Resasco, D. E. *Chem. Phys. Lett.* **2003**, *376*, 302–309.
- (31) Coessens, V.; Matyjaszewski, K. *J. Macromol. Sci., Pure Appl. Chem.* **1999**, *A36*, 667–679.
- (32) Hirsch, A. *The Chemistry of Fullerenes*; Georg Thieme Verlag: Stuttgart, 1994.
- (33) Prato, M.; Li, Q. C.; Wudl, F.; Lucchini, V. *J. Am. Chem. Soc.* **1993**, *115*, 1148–1150.
- (34) Hawker, C. J. *Macromolecules* **1994**, *27*, 4836–4837.
- (35) Huang, X. D.; Goh, S. H. *Macromolecules* **2000**, *33*, 8894–8897.
- (36) Bachilo, S. M.; Strano, M. S.; Kittrell, C.; Hauge, R. H.; Smalley, R. E.; Weisman, R. B. *Science* **2002**, *298*, 2361–2366.

MA035214Q